Journal of Applied Polymer Science

The crosslinking of poly (ether ether ketone): Thermally and by irradiation

Abdul G. Al Lafi,[1] David J. Parker,[2] James N. Hay[3]

[1]Department of Chemistry, Atomic Energy Commission, Damascus, Syrian Arab Republic

[2]The School of Physics and Astronomy, College of Physical Sciences and Engineering, University of Birmingham, Edgbaston, Birmingham B15 2TT, United Kingdom

[3]The School of Metallurgy and Materials, College of Physical Sciences and Engineering, University of Birmingham, Edgbaston, Birmingham B15 2TT, United Kingdom

Correspondence to: A. G. Al Lafi (E-mail: cscientific@aec.org.sy)

ABSTRACT: Crosslinking of amorphous poly (ether ether ketone) films was carried out by means of thermal annealing at 400°C as well as by irradiation with 11.0 MeV proton beam at different dose rate ranging from 1.75 to 15.5 kW g^{-1}. The materials properties of the resulting films were investigated by mean of light microscopy, sol-gel analysis, two-dimensional infra-red correlation spectroscopy, 2DCOS-IR, and differential scanning calorimetry (DSC). It was found that both chain scission and crosslinking yields were decreased by an increase of dose rate and the ratio of crosslinks to chain scission was increased from 0.9 to 1.4. The 2DCOS-IR analysis in the region 1400–1800 cm^{-1} showed progressive development of new bands at 1470 and 1740 cm^{-1}, which have been used to support the presence of crosslinking and chain scission reactions. The glass transition temperature also increased in line with increasing crosslinking density, but the results showed a limiting plateau value for the glass transition T_g, which depended only on the absorbed dose. This suggests that crosslinking was limited and did not increase after a specific value of the dose rate. Crosslinking by irradiation has many advantages over thermal annealing; in particular it is a one step rapid process producing a variety of homogeneously crosslinked, good quality films available for chemical modification. © 2015 Wiley Periodicals, Inc. J. Appl. Polym. Sci. **2015**, *132*, 41999.

KEYWORDS: crosslinking; differential scanning calorimetry (DSC); irradiation

Received 30 September 2014; accepted 16 January 2015

DOI: 10.1002/app.41999

INTRODUCTION

Because of the aromatic nature of the poly (aryl ether ketone)s, with high thermal resistance and toughness, these linear thermoplastics are considered good candidates for a range of applications, especially those which require exposure to hostile environments such as encountered in fuel cells.[1–3] However, excessive osmotic swelling and low-mechanical strength of sulfonated poly (aryl ether ketone)s limit the large scale application of these membranes in fuel cells.[4]

Crosslinking as a route to the preparation of mechanically stable and highly durable polymer electrolyte membranes for fuel cell application has been the subject of several papers.[2,5] For fuel cell application, only a relatively small number of crosslinks are required to produce significant changes in the mechanical properties of polymers and have a profound effect on service life.

While many methods have been developed to crosslink polymers such as PEEK after sulfonation, only few studies have been focused on crosslinking PEEK prior to sulfonation. Although crosslinking the polymer prior to sulfonation leads to diffusion limiting the degree of sulfonation,[6] these methods provide solvent-free procedures for the preparation of polymer electrolyte membrane.

Crosslinking of PEEK has been achieved by different chemical, thermal, and radiation means. In particular, chemical crosslinking has been achieved by chemical means via imine formation at carbonyl groups,[7] but the resultant polymer is stiff and sulfonation has not yet been fully investigated. Another approach that can be used to produce crosslinked PEEK is by annealing the film at elevated temperatures above the melting point.[8,9] However, crosslinking yields were not measured, and one interest in the present work was the evaluation of the crosslink density of thermally annealed PEEK by the modified double log scale model.[10,11] It is important to have a measure of the relative importance of crosslinking and chain scission reactions, which occur simultaneously on thermal annealing. This is due to the fact that crosslinking density affects the thermal, chemical and mechanical properties of the polymers to different extent.

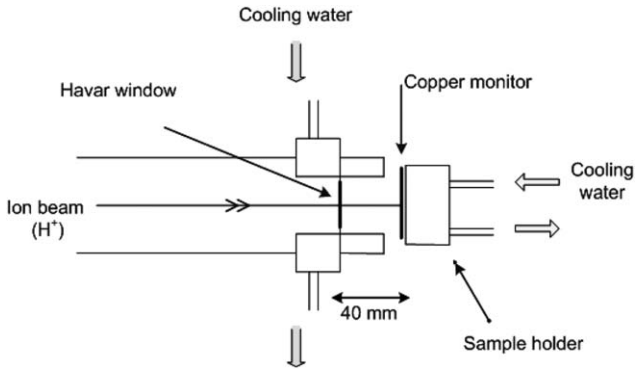

Figure 1. Schematic diagram for the ion irradiation equipment.

Another interest of the present work was the investigation of the efficiency of proton irradiation conditions to optimize polymer modifications and reduce the cost of the final product. In our previous works, irradiations with ions as a route for preparing crosslinked PEEK have been discussed and the materials properties of the resultant materials have been investigated in details.[3,6,12–17] Comparing with helium irradiation, proton irradiation has the advantage of enabling more PEEK layers to be irradiated with different absorbed dose at the same time. In addition, proton irradiation has extensively larger linear energy transfer (LET) values compared with MeV electrons and γ-rays. It has been reported that high-LET increases the radiation yield of crosslinking and decreases that of chain scission.[18] However, to the author's knowledge, no study has been carried out on the effect of dose rate on irradiating PEEK with proton beam at relatively small absorbed doses, that is, below 20 MGy. The dose rate has been shown to alter the net irradiation damage of polymers[19–21] and will be used here as a method to overcome the serious drawback of ion irradiation, that is, high cost, in particular with using aromatic high resistant polymers such as PEEK.

The effects of these conditions on the crosslink density of PEEK will be discussed and the physical properties of the crosslinked films produced thermally and by irradiation will be compared.

EXPERIMENTAL

Materials

Amorphous PEEK was obtained from Goodfellow, the United Kingdom, as a 100 μm thick film with a density of 1260 kg m^{-3}. Gel permeation chromatography gave average molar mass values of 41 kg mole^{-1} and 13 kg mole^{-1} for M_w and M_n, respectively.[14] Methane sulfonic acid (MSA) was obtained from Sigma-Aldrich and used as received, as a solvent and swelling agent.

Crosslinking of PEEK Films: Irradiation Approach

Irradiation was carried out using the University of Birmingham's Scanditronix MC40 Cyclotron. As shown in Figure 1, proton beams of 11.7 MeV having different currents in the range of 100–500 nA were extracted from the cyclotron into air through a 30 µm *Havar* window. The beam was defocused on to a spot size of approximately 10 mm in diameter and scanned over an area of up to 1.8×10^{-4} m^2 by applying saw-tooth waveforms to the inputs of a pair of steering magnets. A stack of foils (10 films) was mounted in air, approximately 10 mm behind the window, in a water-cooled holder to minimize the heat produced on irradiation at high dose rates.

Allowing for the energy lost in the *Havar* window and the air gap, the energy of the protons incident on the first foil was calculated to be 11.0 MeV. For each irradiation, the total charge was fixed at 6.0×10^{-4} C, and the total proton fluence was determined by measuring the ^{65}Zn activity produced in the copper monitor foil as described earlier.[12] This was found to be 3.33 C m^{-2}. The time of irradiation and the beam current were varied to enable the samples to be irradiated to the same doses but with different dose rates. The beam currents were in the range 100 to 500 nA and the exposure times varied from 20 to 100 min. This allowed for dose rates ranging from 1.75 to 15.5 kGy s^{-1}.

The track density value was 20.8×10^{18} ions m^{-2}, which indicates that the dose delivered is concentrated in narrow parallel tracks passing through the foils. The average track spacing value was 2.35×10^{-10} m, which shows that in the present study the damage tracks effectively overlap to cover the entire irradiated area.

The absorbed dose, D (MGy), was calculated using the following equation:[3]

$$D = S \times \frac{Q}{Z_{\text{inc}}} \quad (1)$$

where S is the mass stopping power of the material (MeV m^2 kg^{-1}), Q is the fluence (C m^{-2}), and Z_{inc} is charge number of incident ion. The absorbed dose of the first PEEK layer was calculated from the incident energy and that of the other PEEK layers was calculated based on the inlet energy after the ions passed through the previous layers. The absorbed doses varied in the range 10.5 ± 2.5 MGy at the first layer to 18.1 ± 2.5 MGy at the final layer.

Crosslinking of PEEK Films: Thermal Treatment

Crosslinking of PEEK samples was also carried out by annealing at temperature of 400°C and for different periods ranging from 0.5 to 24 h. Amorphous PEEK film samples were placed in an aluminium foil holder and annealed in an air atmosphere using a Pyro thermal furnace. At the end of each annealing experiment the samples were quenched immediately in liquid nitrogen to produce amorphous PEEK.

Gel Contents

The gel content of the irradiated films was determined by extracting with MSA, which has been reported as a non-sulfonating solvent for PEEK even after 1 week in contact with it.[22,23] The extraction procedure was carried out by immersing weighed samples (≈10 mg) in 10 cm^3 of MSA at room temperature for 24 h. At the end of this period, the solvent was decanted, the gel remaining was thoroughly washed in distilled water and methanol, and left to dry in air for 24 h and in a vacuum oven for at least 12 h at 60°C before finally being weighed.

Differential Scanning Calorimetry

Thermal properties of the PEEK samples were measured using a Perkin-Elmer differential scanning calorimeter DSC-7. Experiments were carried out in an argon atmosphere at a flow

rate of 20 cm^3 min^{-1} and heating rate of 20°C min^{-1}. Heating scan was performed from 50 to 360°C and the glass transition temperature, T_g, was determined from the midpoint of the inflection of the specific heat plot with temperature, using PYRIS software. Temperature and enthalpy calibrations were carried out using ultra pure metal standards: indium (m.p: 429.78 K, $\Delta H = 29.2$ J g^{-1}), tin (m.p: 505.06 K), and lead (m.p: 600.65 K).

Microscopy

An incident light microscope (Leica DM LM; Leica Microsystems Imaging Solutions, Cambridge, UK) with a 100 W halogen illumination, a digital camera and a computer was used to investigate the surface properties of the PEEK films. All images were photographed at 125x objective magnification.

Infrared Spectroscopy and 2D Correlation Analysis

A Nicolet Magna-IR 860 FTIR spectrophotometer operating with the Golden Gate Accessory as an attenuated total reflectance (ATR) attachment and a DTGS detector was used. All spectra were collected from 650 to 3800 cm^{-1} at a resolution of 2 cm^{-1} and a total of 200 scans. A separate background spectrum was subtracted for each spectrum, and all spectra were baseline corrected using OMNIC software, smoothed with a Savitzky–Golay smoothing function of two polynomials and 13 points. ATR technique measures the surface layer of the film which in this study was an advantage as PEEK strongly absorbed the proton radiation. To get physical significance on a molecular level, the ATR spectra were further processed by normalizing them to the same thickness based on the intensity of the 1600 cm^{-1} band, as reported earlier.[17]

The subsequent 2D correlation analysis was performed using the algorithm developed by Noda,[24,25] and calculated using the 2DShige version 1.3 software (Shigeaki Morita, Kwansei-Gakuin University, 2004–2005). The spectral intensity of each sample was corrected by subtracting a reference spectrum taken as the spectrum of the sample with maximum dose rate. The 2D correlation spectra consist of positive (shown in white or red areas) and negative (shown in gray or blue areas) cross-peaks in both synchronous and asynchronous maps, and they are interpreted by means of Noda's rule.[25]

RESULTS AND DISCUSSION

Sol-Gel Analysis of Irradiated PEEK

Figure 2 shows the progressive increase in gel content with dose on irradiating amorphous PEEK with proton beams at different operating current. There was a progressive increase in gel content with increasing dose and beam current. The gel content appeared to level off at the highest dose and beam current with a maximum at about 60 ± 5% at an absorbed dose of 18.1 MGy.

These results are consistent with the reported gel analysis on proton irradiated PEEK[3,14] and confirmed that ion beam current had an effect on the final yield of crosslinking, for comparison, at 10 MGy and with beam current of 40 nA, the gel content was reported to be 13%,[14] and at the same dose but using a higher current of 200 nA the gel increased to 23%.[3]

There are many means of quantifying the relative importance of crosslinking to chain scission in the proton irradiation of PEEK

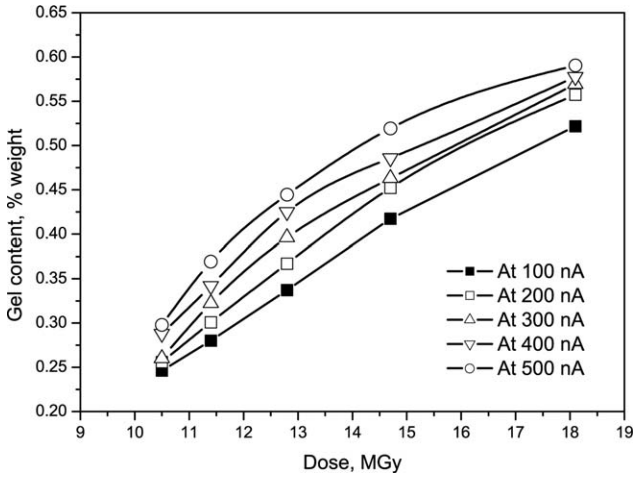

Figure 2. The increase in gel content of PEEK on irradiation with proton beam of different current, plotted as a function of dose.

these include the Charlesby–Pinner and the Charlesby–Rosiak as well as a double log analytical procedure. In the Charlesby–Pinner method, the solubility of the polymer, S, is plotted against the inverse of the dose, $1/D$, in accordance with the following equation:

$$s+\sqrt{s}=\frac{p_0}{q_0}+\frac{2}{q_0.u.D} \tag{2}$$

in which q_0 is the cross link density (the proportion of cross links) per unit irradiation dose, P_0 is the ratio of main chain breaks per unit irradiation dose, and u is the initial weight average degree of polymerization. This equation applies only to polymers having a random initial molecular weight distribution and predicts a linear relationship between $(s+\sqrt{s})$ and $1/D$.[26]

The Charlesby–Rosiak model operates with a virtual irradiation dose, D_V the value of which is varied until the corresponding plots become rectilinear. It is given by the following equation:[27]

$$s+\sqrt{s}=\frac{p_0}{q_0}+\left(2-\frac{p_0}{q_0}\right)\left(\frac{D_V+D_g}{D_V+D}\right) \tag{3}$$

In selecting the best virtual dose value, special software (GelSol 95)[28] was used and the results expressed as irradiation yield versus beam current. As can be seen, in Figure 3, there is agreement at low-beam current but the results were scattered at the highest beam currents, indicating that the Charlesby–Pinner model was not suitable to describe the relation between solubility and absorbed dose. However, the Charlesby–Rosiak equation predicts an increase in crosslinking at higher beam current.

Another method which has been developed to overcome the shortcoming of the Charlesby–Pinner equation is the double log method of analysis.[10,11] In this a plot of the logarithm of the solubility against the logarithm of the irradiation dose is used to determine crosslink and chain scission yields at the gel point with high accuracy. From Figure 4(a) it can be seen that linear plots were obtained from the data displayed in Figure 2 and since

$$\log(s)=a+b\log(D) \tag{4}$$

a and b were determined from the intercept and the slope of a least square fit of the data. Their values are listed in Table I

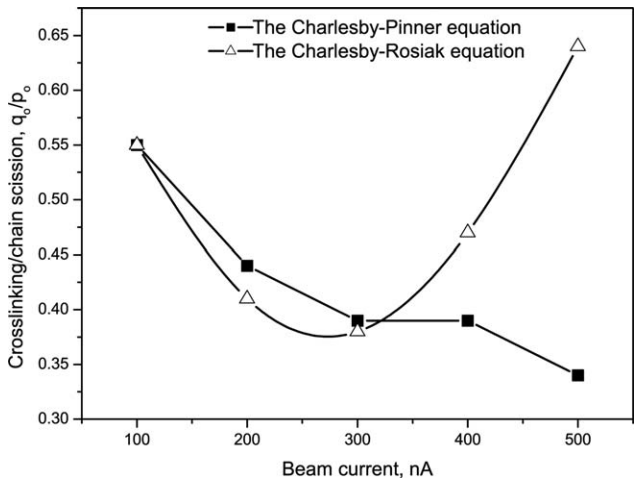

Figure 3. The effect of beam current on the irradiation chemical yield in PEEK according to the Charlesby–Pinner, and the Charlesby–Rosiak equations.

along with the degree of fit, R. The gel-point dose, D_g, was determined by interpolating of the lines to $\log(s)=0$. The values of the slope, b, were used to evaluate the ratio of chain scissions to crosslinking, λ, taking into consideration the initial polydispersity of PEEK, that is, 3.15. These values of λ were in turn used to evaluate the crosslinking index CI_g at the gel point from computer simulations reported in the literature.[10] The corresponding plot for PD = 3.15 was estimated with the help of computer program called "Get Data Graph Digitizer version 2.24." A curve was plotted between the two values of PD = 2 and PD = 5, and this was taken to represent PD = 3.15.

Crosslink and chain scission yields, $G(x)$ and, $G(s)$ respectively, were also calculated from the following equations:

$$G(X)=\frac{CI_g}{M_n D_g} \tag{5a}$$

$$G(S)=G(x)\lambda \tag{5b}$$

where M_n is the number average molecular weight of PEEK.

The resultant values of D_g, λ, CI_g, $G(X)$, and $G(S)$ are quoted in Table I. The low values of both $G(X)$ and $G(S)$ indicate that PEEK is highly resistant to damage by irradiation. The values also decreased with increasing beam current. The ratio of crosslinking $G(X)$ to chain scission $G(S)$ signifies the increasing importance of crosslinks to chain scissions, and it is a measure of the net irradiation damage to the polymer[26,29]; this increases with beam currents as can be seen in Figure 4(b).

Similar results have been reported on the effect of dose rate of γ-rays irradiation on different types of insulating polymers.[19,20] The effect of dose rate has been shown to be dependent on the rate of oxygen diffusion, solubility of oxygen in the target material and the G values of radical formation and their subsequent rate of breakdown.[21] PEEK is highly resistance to permeation and diffusion of gases due to its morphology and degree of crystallinity. The permeability, diffusion, and solubility coefficients on PEEK films for oxygen have been found to be independent of applied upstream pressure and thickness.[30] It has been also reported that diffusion coefficient was reduced with increasing crosslinking density.[13] Based on these the following conclusion could be made: At high dose rates, the atmospheric oxygen is consumed on the surface before it diffuses to the centre of the polymer and degradation will occur heterogeneously and not homogeneously. At lower dose rates, oxidation is homogeneous and the hydroperoxides produced decompose as a function of time to free radicals. These continue to react with oxygen and further degradation occurs.[19–21]

The results imply that an effective cost reduction in the crosslinking process of PEEK membranes of at least five folds can be achieved by irradiation at higher dose rates. In other words, the time required to prepare a crosslinked PEEK membrane using proton irradiation can be shortened by increasing the beam current of the incident radiation. Moreover, the penetration range of 11.0 MeV protons ions into amorphous PEEK was approximately 1.2 mm.[3] Therefore a stack of 10 PEEK foils, each 100 μm thick, covers almost the entire energy range for 11.0 MeV proton beam and can be irradiated at the same time resulting

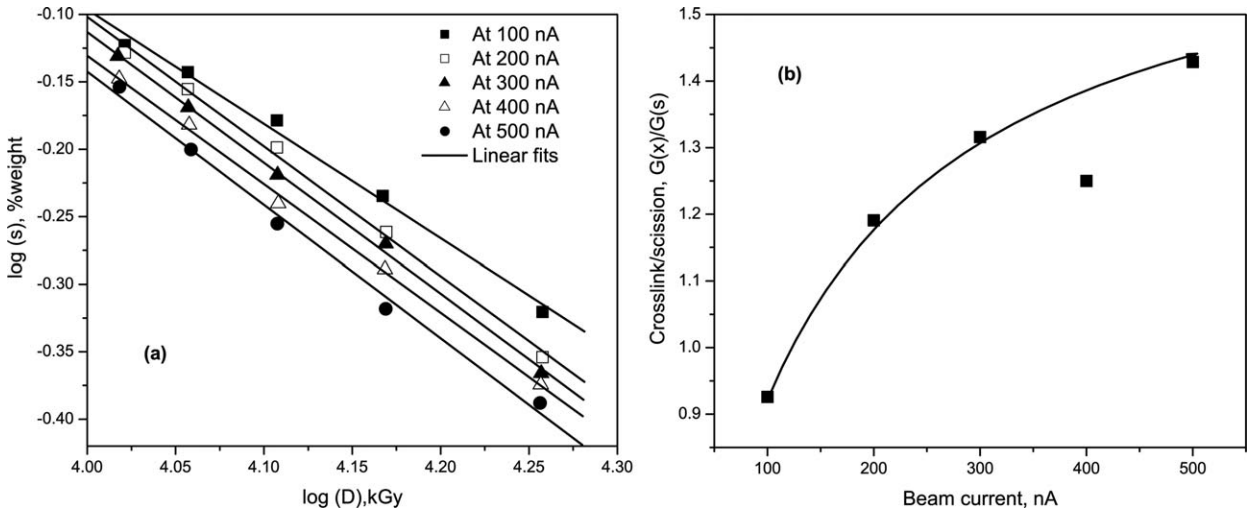

Figure 4. (a) Dependence of solubility on dose during proton irradiation of PEEK Plotted as log (s) vs. log (D) and (b) the effect of beam current on the irradiation chemical yield in PEEK according to the log–log method.

Table I. Sol-Gel Analysis of Proton Irradiated PEEK, The Log–Log Scale Model

							Event per 100 eV	
Beam current (nA)	a	b (kGy^{-1})	R	D_g(kGy)	λ	Cl_g	$G(X)$	$G(S)$
100	3.30	−0.85	0.996	7600	1.08	3.47	0.034	0.037
200	3.75	−0.96	0.998	8000	0.84	3.15	0.029	0.025
300	3.77	−0.99	0.999	6400	0.76	3.04	0.035	0.027
400	3.68	−0.95	0.999	7500	0.80	3.11	0.031	0.025
500	3.81	−0.99	0.997	7100	0.70	2.92	0.031	0.022

in further cost reduction. Although different crosslink densities will be produced this will not have any negative effect on the sulfonation reaction, the final water uptake and mechanical properties of the membranes.[6,13]

The Effect of Dose Rate on Thermal Properties

To determine the best model for sol-gel analysis, DSC experiments were carried out to determine the values of the glass transition temperature of the irradiated samples. Figure 5(a) shows the dependence of the glass transition, measured from the first heating scan, of irradiated PEEK films on the dose rate. At each absorbed dose, there was a slight increase in the measured T_g with increasing dose rate. These results are consistent with the increasing constrain on the chain segments due to network formation and increasing cross link density but was inconsistent with chain scission, thus, justifying the double log model as the best fitting procedure for the gel data in this work.

However, as can be seen form Figure 5(a), there was a limiting plateau value for T_g, which depends on the absorbed dose. This was at 147.3 and 148°C at doses of 10.5 and 18.1 MGy, respectively.

Crosslinking and degradation by chain scission are two competing reactions, which accompany radiation. The ratio of the G values for crosslinking $G(X)$ to chain scission $G(S)$ can be used to indicate which process is dominant. Although $G(X)$ and $G(S)$ both change with radiation conditions such as the absorbed dose, the temperature, and atmosphere, it is reasonable, in the present case, to attribute the plateau shape of the relation between T_g and dose rate to the effect of increasing temperature, which accompany the increase of the dose rate. This would result in increasing the chain mobility, which favors crosslinking but at the same time would increase the oxygen diffusion through PEEK films, and as a consequence more chain scission reactions. T_g values levels off because an equilibrium was reached between these two competing effects. To account for the variation in the absorbed dose, T_g values were plotted in Figure 5(b) as a function to the normalized radiation chemical yield, $D \times G(X)/G(S)$, which can be used as a measure of the crosslinking density. As expected, a linear relation was observed. This was consistent with the literatures.[14,31]

2D-IR Correlation Spectroscopic Analysis

Figure 6(a) shows the FTIR spectra of irradiated PEEK with proton beam having different current in the finger print region. On irradiation, a progressive yellowing of the polymer film with increasing dose rate was observed. This was attributed to the development of new bands at 1720–1735 cm^{-1}, and assigned to the production of new carbonyl species,[17,32–34] produced by the reaction of radicals with molecular oxygen and subsequent decomposition of the peroxy radicals. These minor bands, Figure 6(b), were of very low intensity due to the fact that PEEK possesses high resistance to irradiation, and the number of new chemical bonds formed was small even at high dose

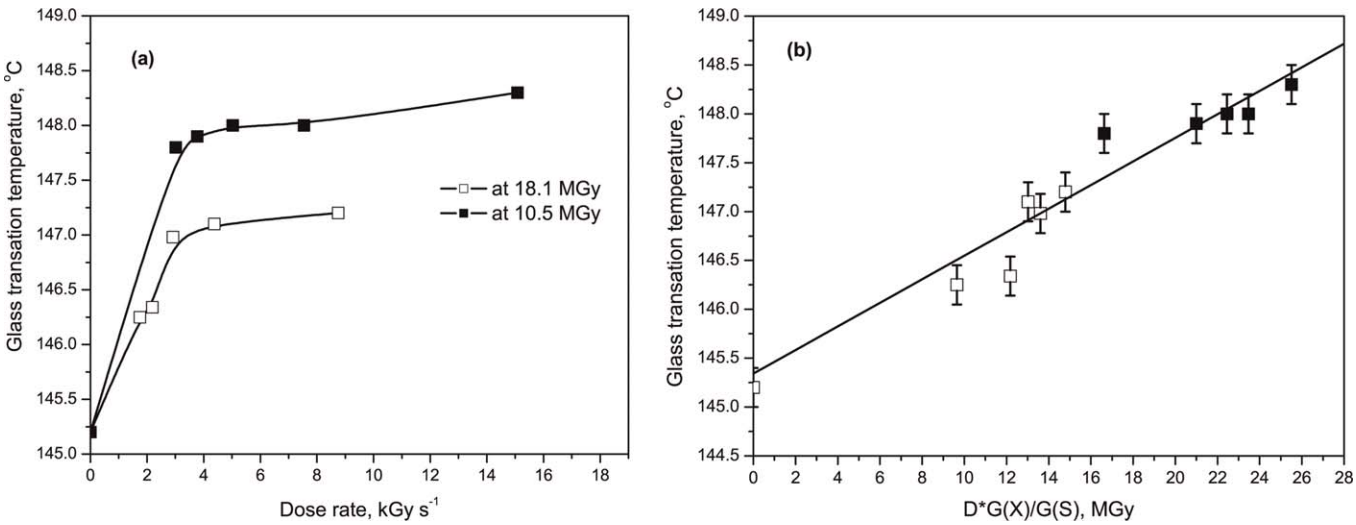

Figure 5. The effect of (a) dose rate and (b) crosslink to chain scission ratio on the glass transition of proton irradiated PEEK.

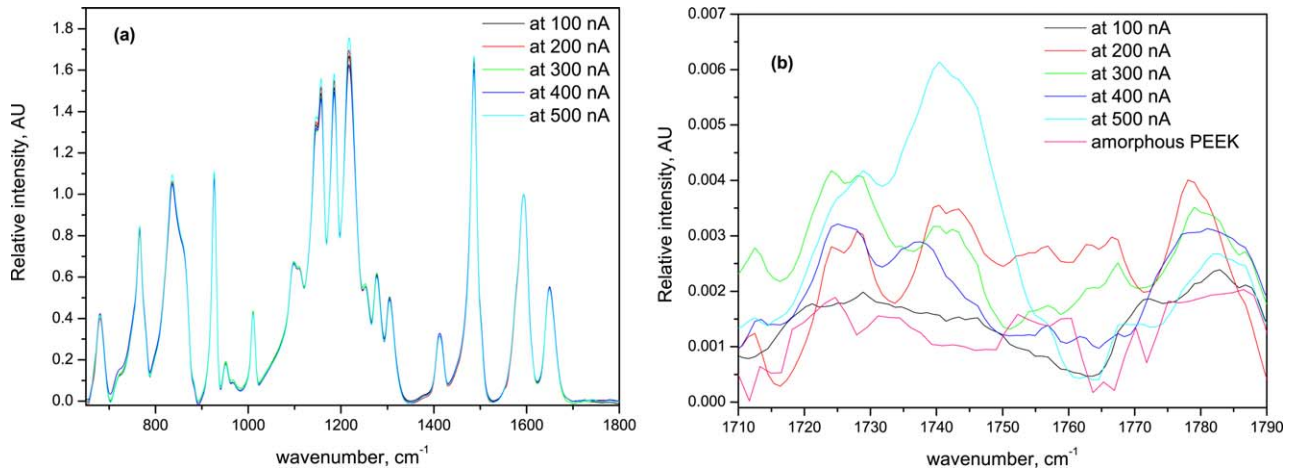

Figure 6. The FTIR spectra of proton irradiated PEEK in the fingerprint region (a) and in the region 1700–1800 cm^{-1} (b). Beam current in the range 100–500 nA. [Color figure can be viewed in the online issue, which is available at wileyonlinelibrary.com.]

rates. 2D correlation spectroscopy was used to investigate the effect of dose rate on these minor bands.

The effects of absorbed dose on ion irradiation of PEEK have been discussed extensively previously,[17] and we focus in the following discussion on the effects of proton beam current only, that is, samples irradiated to the same dose but at different dose rate in the range 1.75 to 15.5 kW g^{-1}. It has been reported that the region 1800–1400 cm^{-1} of the IR spectrum of PEEK could be used to obtain information about the different irradiation effects and thus it will be considered.

The 2D maps of the proton irradiated PEEK in the region 1800–1400 cm^{-1} are shown in Figures 7(a,b). The synchronous spectrum of Figure 7(a) reveals the presence of auto-peaks at 1505, 1485, and 1470 cm^{-1}, negative cross-correlation peaks at 1485 cm^{-1} decreasing in intensity, with the other bands at 1650, 1600, 1505, 1470, and 1415 cm^{-1} and positive cross-correlation peaks at (1630, 1485) and (1505, 1470) cm^{-1}. These suggest that the bands at 1630, 1485 cm^{-1} change in the same direction but in the opposite direction to the bands at 1650, 1600, 1505, 1470, and 1415 cm^{-1}.

The upper side of the asynchronous spectrum of Figure 7(b) shows the most important asynchronous cross-peaks. These were the positive cross-peaks at (1735, 1485), (1630, 1485), and (1505, 1460) cm^{-1} and the negative cross-peaks at (1650, 1485) and (1485, 1460) cm^{-1}.

The signs of the cross-peaks indicates that the intensity increase of the band at 1650 cm^{-1} occurs earlier than the decrease in intensity at 1485 cm^{-1} and the intensity decrease at 1630 cm^{-1}

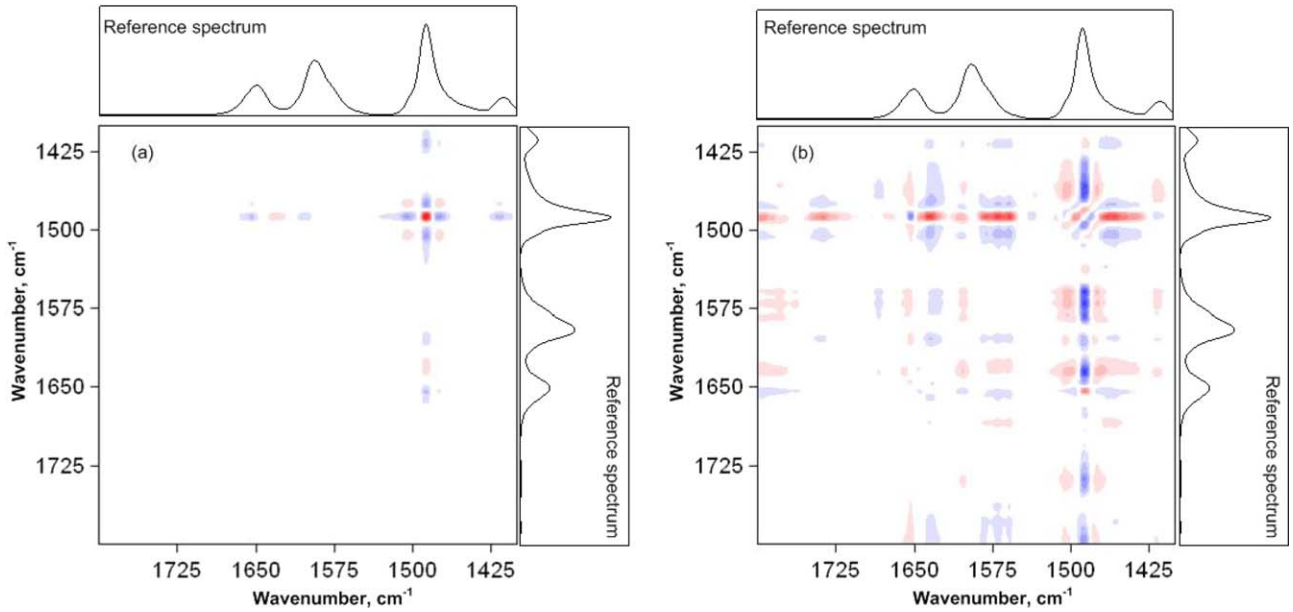

Figure 7. The 2D correlation maps of proton irradiated PEEK with different dose rate, in the region 1800–1400 cm^{-1}. (a) and (b) synchronous and asynchronous maps. Red (or white) and blue (or gray) areas represent negative and positive correlation, respectively. [Color figure can be viewed in the online issue, which is available at wileyonlinelibrary.com.]

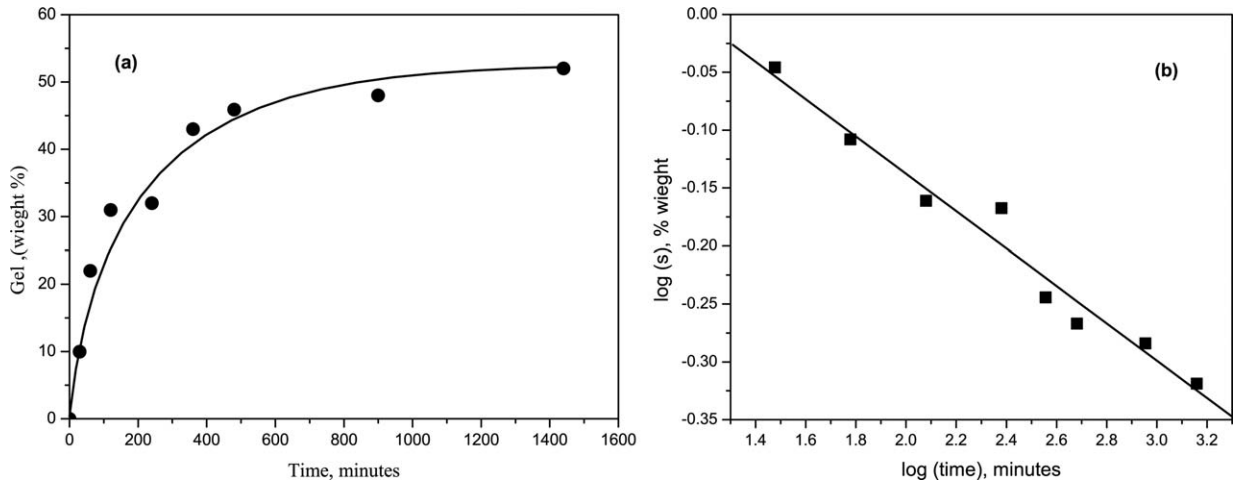

Figure 8. Experimental data on thermal annealing of PEEK at 400°C plotted as gel content versus time (a) and log (s) versus log (time) (b).

occurs before the decrease at 1485 cm^{-1}. The increase in carbonyl intensity may be explained as due to the increase number of non-bonded carbonyl groups as a result of raised temperature due to increasing dose rate.

The most important changes which occur to the carbonyl region are the progressive development of distinct new band at 1735 cm^{-1} and the decrease in the band at 1630 cm^{-1}. The band at 1630 cm^{-1} is characteristic for hydrogen bonds of carbonyl stretching vibration but may be due to the presence of α-hydroxyl diarylketone.[17,33,35] This suggests that irradiated PEEK losses water due to the thermal effect of increasing the beam current. The bands at 1735 cm^{-1} are attributed to oxidation products as observed in thermal degradation and FT-IR studies.[36] The bands at 1485 and 1500 cm^{-1} are attributed to the skeletal vibration of aromatic ring. The 1485 cm^{-1} band is strong in intensity and is sensitive to the number and nature of the ring substituent.[33,35] It decreased with increasing irradiation dose rate and split to form new band at 1470 cm^{-1} characteristic of three substituted aromatic ring.[35]

In conclusion, the 2DCOS-IR analysis provides structural evidence that both crosslinking and chain scission accompany irradiation. It is noteworthy that increasing the absorbed dose[17] resulted in two new carbonyl bands at 1720 and 1735 cm^{-1} but with increasing the dose rate, at constant absorbed dose, only the most stable band is present, that is, the band at 1735 cm^{-1} which is attributed to an aromatic ester group.

Sol-Gel Analysis of Thermally Annealed PEEK

Figure 8(a) shows the progressive increase in gel content with time on annealing amorphous PEEK at temperature of 400°C. The choice of temperature was based on the literature.[9] Prolonged annealing in air resulted in a marked increase in the gel content and in particular within the first 6 h. The gel content was observed to level off at about 50% with increasing annealing time up to 24 h. This behavior indicates that the effect of thermal annealing in air on amorphous PEEK occurs predominately by a crosslinking process. As knowledge of the crosslinking density was of prime importance, the double log scale analysis was used to evaluate the crosslinking yield in the thermal annealing of PEEK. From Figure 8(b) it can be seen that a linear plot was obtained from increase in gel content with time as displayed in Figure 8(a) implying that

$$\log(s) = a + b\log(t) \tag{6}$$

Following the analysis, as detailed above for the irradiated samples, the best fit was obtained with a regression coefficient $R = 0.984$ and gave values of 0.185 and −0.161 for a and b, respectively. The corresponding values of λ and CI_g were 2.98 and 0.71, respectively, and crosslink and chain scission yields were calculated from eqs. (5a and 5b) after replacing the gel dose with gel time in eq. (5a). It was noted that the value of chain scission was higher (1.94×10^{-8} mole kg^{-1} s^{-1}) than that of crosslinking (6.5×10^{-9} mole kg^{-1} s^{-1}) and different from the values obtained from irradiation. The ratio $G(X)/G(S)$ was found to be 0.33, which was consistent with the production of volatile compound on thermal annealing of PEEK as reported.[36]

The Characteristics of Crosslinked Samples

Figure 9(a–c) shows an optical micrograph of PEEK films taken at 125x magnification. Irradiation with high beam current without cooling the samples resulted in brown films containing bubbles (due to the evolution of volatiles) and an increase in temperature above the glass transition. This is shown in Figure 9(c), and the films produced did not dissolve in MSA. Thermal effects can give rise to an increase in the crosslink yield, $G(X)$, which is to be expected if the sample temperature exceeds the glass transition of the target materials.[37] For PEEK with a glass transition value of 145°C and at the dose rates used in this work, that is, 1.75–15.5 kW g^{-1} an increase in the sample temperature to above the transition temperature is possible. To avoid any significant increase in the sample temperature and so to reduce the contribution of thermal effect in gel analysis, water-cooled jacket was inserted into the radiation holder. Its effectiveness was examined by inspection of the samples after irradiation. As shown in Figure 9(b), there was no evidence of crystallisation or bubble formation on PEEK films irradiated using water cooling, but they were discoloured by the beam. In fact, samples irradiated even with the lowest dose rate and with cooling were discolored.

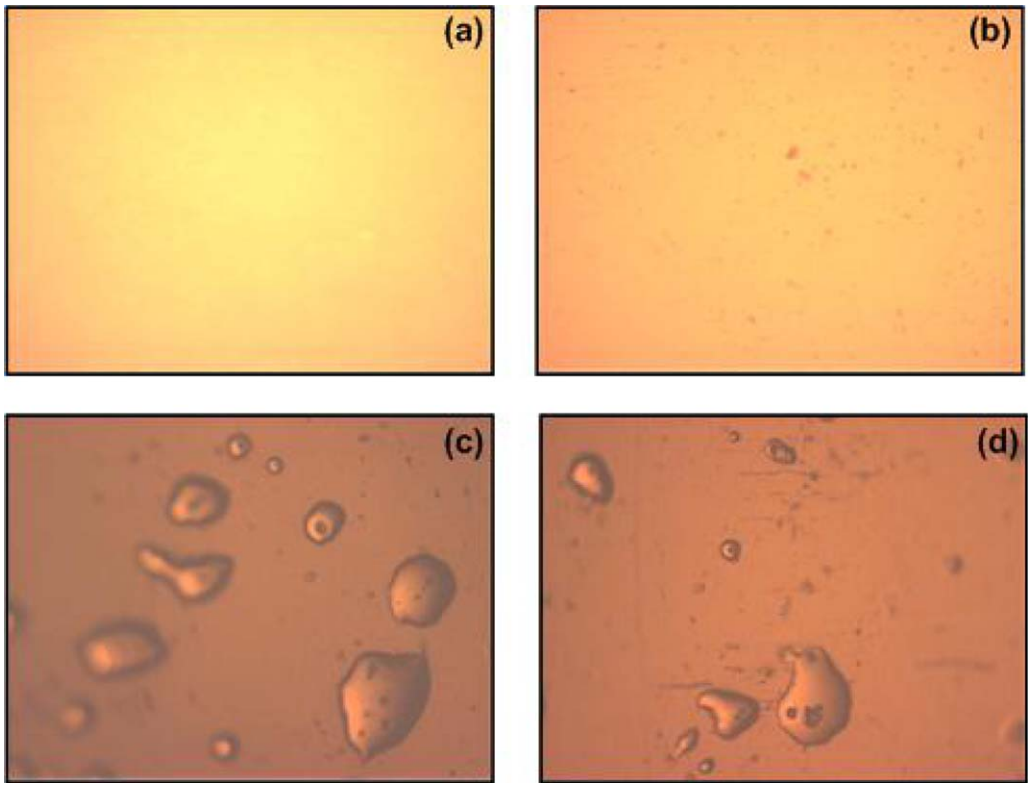

Figure 9. PEEK films light micrographs 125x magnification. (a) Amorphous un-irradiated, (b) and (c) irradiated (12.8 MGy with 500nA proton beam) films, with cooling (b) and without cooling (c), and (d) thermally treated film at 400°C for 6 h. [Color figure can be viewed in the online issue, which is available at wileyonlinelibrary.com.]

One of the problems encountered with the thermal treatment of PEEK films was that the films stuck to the surface of the carrier materials (aluminium foils) and required further treatment with alkali to remove these foils. Another problem was that quenching the molten samples into liquid nitrogen to obtain amorphous samples introduced mechanical stresses. In addition, bubbles were produced within the film due to the evolution of volatiles and the high viscosity of the molten films, as shown in Figure 9(d). These will result in defects in the films after sulfonation.

In comparison, irradiation provides a fast and clean one step process for the preparation of crosslinked membranes, providing that the proper irradiation setup are used such as water cooling. Moreover, due to the more complex reactions that accompany irradiation, the irradiated materials will have attached polar groups. These polar groups would increase the rate of sulfonation and resulted in improved materials properties as reported.[6,13,17]

CONCLUSIONS

Thermal annealing at 400°C as well as proton irradiation with 11.0 MeV beam at different dose rate were investigated as routes to crosslink amorphous poly (ether ether ketone) films. Irradiation was more effective as evident from $G(X)/G(S)$ values of 0.92 to 1.43 on irradiation with different dose rate compared to 0.33 on thermal annealing at 400°C. Although crosslinking increased at higher dose rate this was limited as shown by the plateau value of the glass transition temperature, which in turn depends on the absorbed dose.

The analysis with 2D-COS-IR showed that increasing the dose rate resulted in similar effects to increasing the absorbed dose, but differences were observed at the molecular level. The absorbed dose had more effect in producing these changes and thermal effects played a more important role with increasing the dose rate.

Crosslinking by irradiation has many advantages over thermal and these includes the one step process on preparing variety of controlled and homogeneous crosslinked PEEK film, shorter time and better quality films for further chemical modification. To overcome the disadvantage of the high cost of irradiation two methods were suggested: Increasing the dose rate which reduces the total time of irradiation, and stacking PEEK films which allows the projected range of proton beam in PEEK to be covered. These two methods can be used to optimize irradiation techniques and reduce the total cost of irradiation. Membranes with a range of crosslink densities were obtained and were suitable for further chemical modification to produce mechanically stable polymer electrode membranes.

ACKNOWLEDGMENTS

The authors thank Professor I. Othman, the General Director of the AEC of Syria and Professor Z. Ajji, the Head of Chemistry Department for their encouragements. Thanks are also due to Frank Biddlestone and Alaa Hjazy for their technical assistance.

REFERENCES

1. Kreuer, K. D. *J. Memb. Sci.* **2001**, *185*, 29.
2. Sopian, K.; Daud, W. R. W. *Renew. Energ.* **2006**, *31*, 719.
3. Al Lafi, A. G.; Hay, J. N.; Parker, D. J. *J. Polym. Sci. Part B: Polym. Phys.* **2008**, *46*, 1094.
4. Alberti, G.; Casciola, M.; Massinelli, L.; Bauer, B. *J. Memb. Sci.* **2001**, *185*, 73.
5. Kreuer, K. D. *Solid State Ionics* **1997**, *97*, 1.
6. Al Lafi, A. G.; Hay, J. N. *J. Polym. Sci. Part B: Polym. Phys.* **2009**, *47*, 775.
7. Thompson, A.; Farris, R. J. *J. Appl. Polym. Sci.* **1988**, *36*, 1113.
8. Day, M.; Cooney, J. D.; Wiles, D. M. *J. Appl. Polym. Sci.* **1989**, *38*, 323.
9. Day, M.; Sally, D.; Wiles, D. M. *J. Appl. Polym. Sci.* **1990**, *40*, 1615.
10. Shyichuk, A.; Shyichuk, I. *Macromol. Chem. Phys.* **2002**, *203*, 401.
11. Shyichuk, A.; Tokaryk, G. *Macromol. Theor. Simul.* **2003**, *12*, 599.
12. Al Lafi, A. G. *Polym. Bull.* **2012**, *68*, 2269.
13. Al Lafi, A. G.; Hay, J. N. *J. Appl. Polym. Sci.* **2013**, *128*, 3000.
14. Al Lafi, A. G.; Hay, J. N.; Parker, D. J. *J. Polym. Sci. Part B: Polym. Phys.* **2008**, *46*, 2212.
15. Al Lafi, A. G. *Polym. Adv. Technol.* **2014**, *25*, 9.
16. Al Lafi, A. G. *J. Appl. Polym. Sci.* **2014**, *131*, 2593.
17. Al Lafi, A. G. *Polym. Degrad. Stab.* **2014**, *105*, 122.
18. Sasuga, T.; Kudoh, H. *Polymer* **2000**, *41*, 185.
19. Gillen, K. T.; Clough, R. L. *Radiat. Phys. Chem.* **1981**, *18*, 679.
20. Reynolds, A. B.; Bell, R. M.; Bryson, N. M. N.; Doyle, T. E.; Hall, M. B.; Mason, L. R.; Quintric, L.; Terwilliger, P. L. *Radiat. Phys. Chem.* **1995**, *45*, 103.
21. Sasuga, T.; Hagiwara, M. *Polymer* **1987**, *28*, 1915.
22. Bishop, M. T.; Karasz, F. E.; Russet, P. S. *Macromolecules* **1985**, *18*, 86.
23. Bailly, C.; Williams, D. J.; Karasz, F. E.; MacKnight, W. *J. Polymer* **1987**, *28*, 1009.
24. Noda, I. *Appl. Spectr.* **1993**, *47*, 1329.
25. Noda, I.; Ozaki, Y. Two-Dimensional Correlation Spectroscopy: Applications in Vibrational and Optical Spectroscopy; Wiley: Chichester, **2004**.
26. Charlesby, A. Atomic radiation and polymers; Pergamon Press Ltd: London, **1960**.
27. Olejniczak, J.; Rosiak, J.; Charlesby, A. *Radiat. Phys. Chem.* **1991**, *37*, 499.
28. .GelSol 95 is available through the internet from: http://mitr.p.lodz.pl/biomat/gelsol.html.
29. Chapiro, A. Radiation chemistry of polymeric systems (High Polymers V 15); Wiley: New York, **1962**, p 37 and 339.
30. Monson, L.; Moon, S. I.; Extrand, C. W. *J. Appl. Polym. Sci.* **2013**, *127*, 1637.
31. Vaughan, A. S.; Stevens, G. C. *Polym. Commu.* **2001**, *42*, 8891.
32. Lambert, J. B.; Shurvell, H. F.; Lightner, D. A.; Cooks, R. G. Organic structural spectroscopy; Prentice-Hall, Inc.: New Jersey, **1998**.
33. Socrates, G. Infrared and Raman Characteristic Group Frequencies Tables and Charts, 3rd ed. Wiley: England, **2001**.
34. Bellamy, L. J. The Infrared Spectra of Complex Molecules; Chapman & Hall: London, **1975**.
35. Silverstein, R. M.; Webster, F. X.; Kiemle, D. J. Spectrometric Identification of Organic Compounds, 7th ed. Wiley: USA, **2005**.
36. Hay, J. N.; Kemmish, D. J. *Polymer* **1987**, *28*, 2047.
37. Schnabel, W.; Klaumünzer, S. *Radiat. Phys. Chem.* **1991**, *37*, 131.